

Weather-Dependent Transient Stability Analysis of Single-Machine Infinite-Bus System

Arif Ahmed^{*}, Fiona Stevens McFadden[†], Ramesh Rayudu[‡], and Tobias Massier[§]

^{*}[†]Robinson Research Institute, ^{*}[‡]Smart Power and Renewable Energy Systems Group

^{*}[†][‡]School of Engineering and Computer Science, Victoria University of Wellington, Wellington 6140, New Zealand

^{*}[§]TUMCREATE, 1 CREATE Way, #10-02 CREATE Tower, Singapore 138602

Email: ^{*}arif.ahmed@vuw.ac.nz, [†]fiona.stevensmcfadden@vuw.ac.nz,

[‡]ramesh.rayudu@vuw.ac.nz, and [§]tobias.massier@tum-create.edu.sg

Abstract—Stability studies are essential in determining the ability of power systems to overcome disturbances and retain synchronism. To this end, transient stability analysis (TSA) deals with instability due to large disturbances in the power system such as occurrence of faults, loss of generation, line outage, etc. Traditional TSA of single-machine infinite-bus (SMIB) systems relies on equal-area criterion and time-domain simulations based on simplified assumptions without modelling of the weather-dependent characteristics. Weather affects power flow analysis (PFA), and incorporating weather-dependent characteristics improves the accuracy of PFA and consequently impacts TSA by accurately estimating power system states. In this manuscript, the weather-dependent impacts are modelled and considered for TSA of SMIB systems. The impact of the weather on TSA is demonstrated by investigating the two transient stability indicators i.e. the critical clearing angle and the critical clearing time, whilst utilizing a year-long real weather dataset. Simulations carried out demonstrate the impact of weather on TSA of SMIB systems and highlight the significance of incorporating weather in power system transient stability studies.

Index Terms—Transient Stability Analysis, Equal Area Criterion, Weather Dependent Transient Stability Analysis, Single-Machine Infinite-Bus System

I. INTRODUCTION

Transient stability analysis (TSA) is an essential part of power system stability that involves study of the power system following a large/major disturbance (faults, loss of generation, line outage, etc.) [1]–[4]. During a large disturbance, the acceleration of the rotor shaft of a synchronous generator will vary. The dynamics of which are described by the swing equation [1]–[4]. TSA ascertains if the rotor will return to a stable steady-state condition following the clearance of a disturbance resulting in a stable system.

Modern power networks are increasingly being operated close to their stable limits, threatening system security and stability [5], [6]. This means a substantial amount of time-consuming and computationally expensive TSA simulations is needed with detailed system models in order to operate a secure and stable system. As a result, a large effort has been spent in making simulations computationally efficient and faster [5], [6].

Despite the progress made, major blackouts have still occurred in the last decade [5], [7]. Furthermore, stability

of modern power networks having bi-directional power flow capabilities, distributed generation, communication infrastructure, etc. are constantly being threatened and accurate stability analysis incorporating a range of realistic factors is essential for stable and secure operation of the network. This warrants further improvements in the field of power system stability and security, which is the aim of this manuscript.

Traditionally, TSA relies on equal-area criterion and time-domain simulations, which are based on simplified assumptions and the weather-dependent characteristics are not modelled. It is known that the weather affects power flow analysis (PFA) [8]. Incorporating weather-dependent characteristics improves the accuracy of PFA [8] by accurately estimating power system states, which is expected to improve TSA [9].

A handful of studies to improve TSA by considering weather or weather-dependent effects are found in the literature. The authors in [10] propose a temperature-dependent transmission line model and utilise it to highlight the potential impact of conductor temperature on the transient stability of an SMIB system by assuming a predefined conductor temperature (for demonstration) that depends on the weather condition. Various conductor temperatures were considered for calculating the initial power system states for TSA. Then time-domain simulation of the swing equation was performed based on the initial conditions to show the significant difference in critical clearing angle and time [10]. The investigations in [10] reveal that accounting for the conductor temperature alters the fault clearing angle and time, which are important indicators of transient stability and used in protection design. However, the assumption of predefined conductor temperatures and neglecting the use of a heat balance model of conductor in [10] does not yield accurate impact of weather on conductor temperature and hence in TSA. In [9], a first attempt to incorporate weather parameters into TSA of an SMIB system was undertaken utilizing a linear thermal resistance model [11]. In comparison to the conventional approach, changes in the power-angle curve and stability indicators were observed in [9], which varied with the length and type of conductors.

To date, accurate assessment of the impacts of weather conditions on TSA for an SMIB is not present in the existing literature. It is also not clear how significantly and to what extent weather impacts TSA. Furthermore, TSA utilising a

large year-long real weather dataset is also absent. Therefore, in this manuscript, weather-dependent TSA of a SMIB system is undertaken by considering the steady-state heat balance model [12], [13] and a year-long real weather dataset, to incorporate fully the impact of weather conditions. This manuscript, essentially, addresses the gap of an accurate TSA of SMIB systems by fully considering the weather impacts and demonstrates the impact of weather on TSA of an SMIB system via a simulation case study.

Section II of the manuscript presents an overview of the heat balance model of overhead conductors, Section III discusses the weather-dependent TSA approach followed by Section IV, which presents the SMIB simulation study details. Simulation results are presented and discussed in Section V, and the manuscript is concluded in Section VI.

II. HEAT BALANCE MODEL OF OVERHEAD CONDUCTORS

The IEEE Std 738TM-2012 [12] and the CIGRE Technical Brochure 207 [13] present nonlinear heat balance models (steady-state and dynamic) for overhead conductors that relate the weather condition, loading, and conductor characteristics. The steady-state nonlinear heat balance model can be represented as a nonlinear function of multiple parameters and variables as follows:

$$f(m, C_p, R, T_a, T_c, \alpha, Q_s, D, H_e, V_s, W_{\text{angle}}, \epsilon, I) = q_c + q_r - q_s + q_j = 0 \quad (1)$$

with

m	mass per unit length (kg/m)
C_p	specific heat of the conductor material (J/(kg °C))
R	conductor resistance per unit length (Ω/m)
T_a	ambient temperature (°C)
T_c	conductor temperature (°C)
α	solar absorptivity
Q_s	global solar irradiance (W/m ²)
D	conductor diameter (m)
H_e	conductor elevation above sea level (m)
V_s	wind speed (m/s)
W_{angle}	wind incidence angle or direction (°)
ϵ	emissivity of the conductor
I	current flowing in the conductor (A)
q_c	convective heat loss rate (W/m)
q_r	radiative heat loss rate (W/m)
q_s	solar heat gain rate (W/m)
q_j	Joule heat gain rate (W/m)

The convective heat loss rate (q_c) of a conductor is of two types [12], [13]: natural convection (q_{c_n}) and forced convection (q_{c_1} or q_{c_2}). The following equations can be utilised to calculate the convective heat loss rate.

$$\begin{aligned} q_{c_1} &= K_{\text{angle}}[1.01 + 1.35N_{\text{Re}}^{0.52}]k_f(T_c - T_a) \\ q_{c_2} &= 0.754K_{\text{angle}}N_{\text{Re}}^{0.6}k_f(T_c - T_a) \\ q_{c_n} &= 3.645\rho_f^{0.5}D^{0.75}(T_c - T_a)^{1.25} \end{aligned} \quad (2)$$

IEEE Std 738TM-2012 recommends using the largest calculated value of q_{c_1} , q_{c_2} , and q_{c_n} i.e. $\max(q_{c_1}, q_{c_2}, q_{c_n})$ for the

convective heat loss rate at any given weather condition. K_{angle} is the wind direction factor, N_{Re} is the Reynolds number, k_f is the thermal conductivity of air, and ρ_f is the air density in Equation (2). Detailed equations can be referred to in the IEEE Std 738TM-2012 [12].

The radiated heat loss rate (q_r) in Equation (1) is given by the following expression:

$$q_r = \frac{17.8}{100^4} D \epsilon [(T_c + 273)^4 - (T_a + 273)^4] \quad (3)$$

The heat gain rate due to solar radiation (q_s) in Equation (1) is given by [13]:

$$q_s = \alpha Q_s D \quad (4)$$

The heat gain rate due to Joule heating (q_j) in Equation (1) is given by:

$$q_j = I^2 R(T_c) \quad (5)$$

In Equation (5), $R(T_c)$ is the conductor resistance per unit length at the conductor temperature T_c calculated as [12]:

$$R(T_c) = \left[\frac{R(T_{\text{high}}) - R(T_{\text{low}})}{T_{\text{high}} - T_{\text{low}}} \right] (T_c - T_{\text{low}}) + R(T_{\text{low}}) \quad (6)$$

Here, $R(T_{\text{high}})$ is the conductor resistance at a higher temperature while $R(T_{\text{low}})$ is the conductor temperature at a lower temperature ($T_{\text{high}} > T_{\text{low}}$).

The steady-state nonlinear heat balance Equation (1) can be solved to calculate the conductor temperature (T_c) for any amount of power flowing through a conductor under any given weather condition by substitution of the relevant terms from Equations (2)-(6) into Equation (1) and then solving the nonlinear equation. This relationship is utilised in this manuscript to fully incorporate the effects of weather in TSA.

III. WEATHER-DEPENDENT TSA OF A SMIB SYSTEM

An exemplary SMIB system considered for the weather-dependent TSA is depicted in Figure 1. This SMIB system

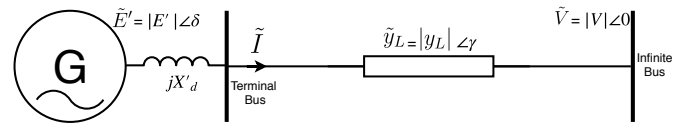


Fig. 1: Single-Machine Infinite-Bus system.

is comprised of a synchronous machine connected to the Infinite-Bus with voltage \tilde{V} (pu) through a transmission line with admittance \tilde{y}_L (pu). The classical synchronous generator model is considered here, which is represented by a constant voltage \tilde{E}' (pu) behind the direct-axis transient reactance X'_d (pu) in the SMIB system [1]–[4]. The complex current flowing in the branch is denoted by \tilde{I} (pu). The SMIB model may be viewed as a transformation of the multi-machine system into a single-machine equivalent system for TSA [14], [15].

To incorporate the impacts of weather conditions in TSA of SMIB systems, the network admittance of the SMIB system model is modified by modelling the weather-dependent effects considering the steady-state nonlinear heat balance model

of overhead conductors presented in the previous section. This means that the line admittance (\tilde{y}_L) in Figure 1 is no longer constant as assumed in traditional TSA, rather it varies depending on the weather conditions.

As TSA involves studying stability of power systems due to large disturbances. The disturbance considered in this manuscript is a three-phase to ground fault. It is found in the literature that broadly, two distinct fault scenarios are investigated for TSA of SMIB systems [1]–[4]. These are:

- 1) *Same pre-fault and post-fault network impedance*: This situation refers to a three-phase fault at the synchronous generator terminal, which is then cleared resulting in the post-fault line impedance being equal to the pre-fault line impedance, and no power flows to the Infinite-Bus during the fault.
- 2) *Distinct pre-fault, post-fault, and during-fault network impedance*: This refers to a fault situation where power flows to the Infinite-Bus during the fault and the network impedance between the synchronous generator and the Infinite-Bus is different in pre-fault, post-fault, and during-fault conditions.

A flowchart representing the weather-dependent TSA methodology is detailed in the following subsection.

A. Flowchart Representation of Weather-Dependent TSA of SMIB Systems

Figure 2 shows a flowchart representing the process of weather-dependent TSA of SMIB systems for both scenarios mentioned before.

The key distinction between traditional TSA and weather-dependent TSA for SMIB systems is the use of weather-dependent pre-fault, during-fault, and post-fault power-angle curves, which make the analysis more accurate. This is achieved by considering the steady-state nonlinear heat balance model of the overhead conductors in the SMIB system to calculate accurate weather-dependent power system states and network impedance.

Initially, after reading all the input data, setting error tolerance, and initialising the power flow and conductor temperature states, the weather-dependent power system states are calculated. This is achieved by first solving a traditional power flow and then calculating the conductor temperatures (Equation (1)) based on the output power system states iteratively. The network impedance is then updated (Equation (6)). This entire process is repeated until the state error tolerance is met, yielding accurate weather-dependent power system states. Since, SMIB systems are small with only two buses, the computational cost of this iterative method is negligible.

After the weather-dependent power system states are solved, the TSA process is followed by calculating the stability indicators i.e. the critical clearing angle (δ_{cr}) and time (t_{cr}) as shown in Figure 2.

IV. SMIB SIMULATION STUDY DETAILS

Simulation study results of only the first scenario (same pre-fault and post-fault network impedance) for Weather-dependent TSA of an SMIB system is presented in this

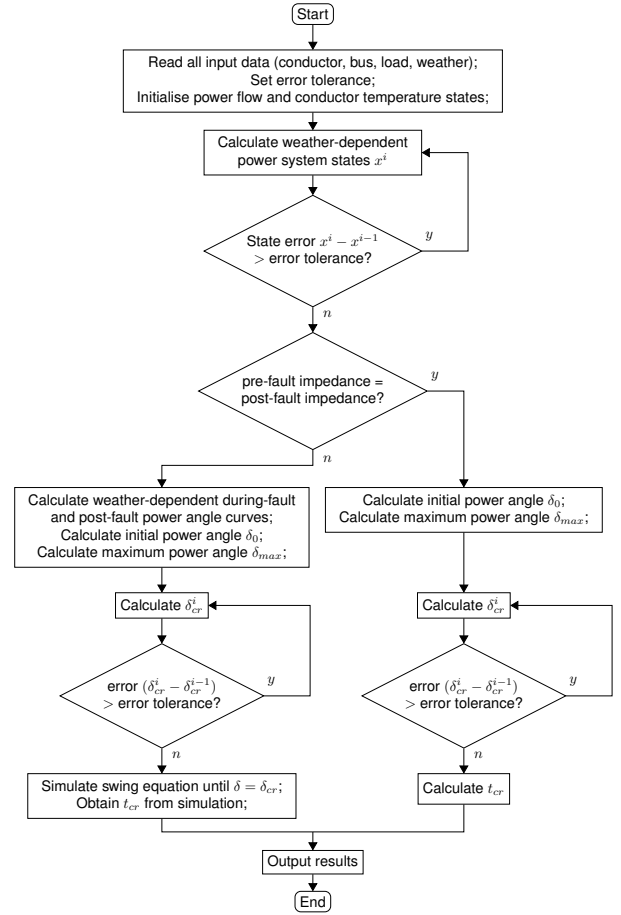


Fig. 2: Flowchart representing the weather-dependent TSA methodology of SMIB.

manuscript. The SMIB system considered for the investigation is presented in Figure 3. The SMIB system is modelled with

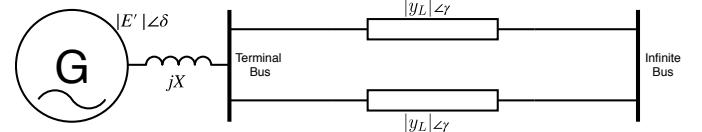


Fig. 3: SMIB model of simulation study.

the inclusion of the steady-state nonlinear heat balance model of the transmission lines as stated earlier. This incorporates the effects of weather conditions in the TSA of the SMIB system. Both transmission lines in Figure 3 are assumed to have the same admittance. The reactance X between the generator and terminal bus represents the sum of the generator's direct-axis transient reactance (X'_d) and the connecting transformer's reactance. The synchronous generator feeds a power of 250 MVA at 0.9 power factor (lag) to the Infinite-Bus. A base power of 100 MVA and a base voltage of 169 kV is considered. The nominal line impedance is $0.0003 + j0.0016$ pu/km at 25°C and is made of the 795 kcmil 26/7 Drake ACSR conductor [8], [12]. The system frequency is 50 Hz and the generator inertia constant H is 9.94 MJ/MVA.

A temporary three-phase to ground fault is simulated which occurs at the terminal bus. The fault is then cleared and both transmission lines are intact.

The length of each transmission line is 80 km. The scenario is simulated considering a year-long real weather dataset of New Zealand utilised in [8].

In addition to investigating the weather-dependent TSA based on the weather data, the effect of loading and transmission line length on the weather-dependent TSA for the scenario is also investigated.

The case study is developed and simulated in MATLAB® and the following assumptions are made:

- The SMIB system in Figure 3 is assumed to be in steady-state before the occurrence of fault.
- Synchronous machine power input is assumed to remain constant throughout the entire period of simulation.
- Damping of the generator is neglected.
- The transmission lines are weather-dependent and experience similar weather conditions throughout the length.
- Emissivity and solar absorptivity of 0.8 is used.

For comparison with the weather-dependent TSA, simulations are also performed using a ‘Nominal impedance’ scenario that considers the transmission lines at nominal line impedance but ignores the weather effects representing a conventional approach to TSA.

V. SIMULATION RESULTS & DISCUSSION

A three-phase to ground fault is introduced in the terminal bus of the generator for every weather condition in the weather dataset of 2016 [8].

The critical clearing angles (δ_{cr}) and times (t_{cr}) as calculated from the TSA are presented in Figure 4. The minimum,

maximum, mean, and range of critical clearing angle and time based on the weather-dependent TSA is presented in Table I.

TABLE I: Min., Mean, Max., and Range of δ_{cr} and t_{cr} based on weather-dependent TSA

	Min.	Mean	Max.	Range
δ_{cr} (°)	92.07	92.32	93.00	0.93
t_{cr} (ms)	279.72	279.92	280.44	0.72

In Figure 4, an important finding is depicted i.e. it is observed that the critical clearing angle and time in the weather-dependent TSA change considerably as the weather conditions change throughout the year. Whilst the critical clearing angle and time obtained for the nominal impedance scenario was 92.15° and 279.78 ms, respectively. The maximum absolute change in critical clearing angle for the nominal impedance scenario was 0.85° and the maximum absolute change in critical clearing time for the nominal impedance scenario was 0.66 ms, when compared to weather-dependent scenario. These differences observed are due to the pre-fault steady-state operating point, which yield different input power and power-angle as a result of the changing line impedance under changing weather conditions. This is explained with clarity later considering Figure 5.

In contrast, the nominal impedance situation does not reflect any change in the critical clearing angle and time as it does not incorporate any impact of changing weather condition. Furthermore, in the weather-dependent TSA, higher critical angles and times are observed as the X/R ratio decreases due to increased conductor temperatures throughout the year. This conforms to the understanding in the literature [16] i.e. a reduction in the X/R ratio causes an increase in the critical clearing time. As the weather condition is observed to impact the critical clearing angle and time, potential power system protection issues are expected e.g. protection devices like the circuit breakers may no longer be confidently set based on stability studies neglecting the effect of weather conditions. Therefore, including the effects of weather on TSA could be significant and will aid in better modeling, analysis, and understanding of the transient stability of power networks.

Since the equal-area criterion for TSA is based on a graphical approach using the power-angle curve, investigating the result via the use of power-angle curves comprehensively describes the results of TSA. A graphical representation of TSA utilizing equal-area criterion is shown in Figure 5 by plotting the power-angle curves for a weather condition on day 35, which yields the highest critical clearing angle and time. In Figure 5, δ_0 is the initial steady-state power angle and δ_{max} is the maximum possible power angle based on the equal-area criterion.

The weather-dependent power-angle curve is observed to have a higher peak and is wider than the nominal impedance scenario resulting in a larger area under the curve. As a result, the weather-dependent critical clearing angle (based on the equal-area criterion) and time calculated for this day is larger. The critical clearing time calculated for the weather-dependent TSA for the weather condition was 280.44 ms.

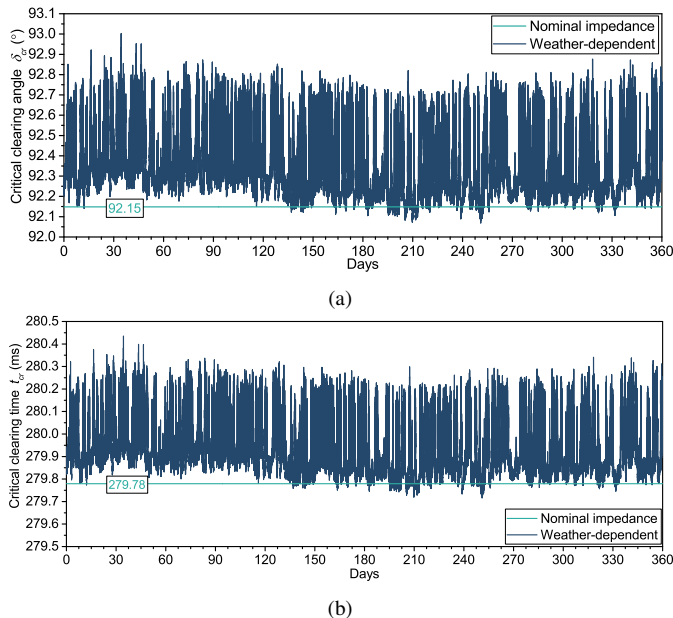


Fig. 4: Critical clearing angle (a) and time (b) throughout the year.

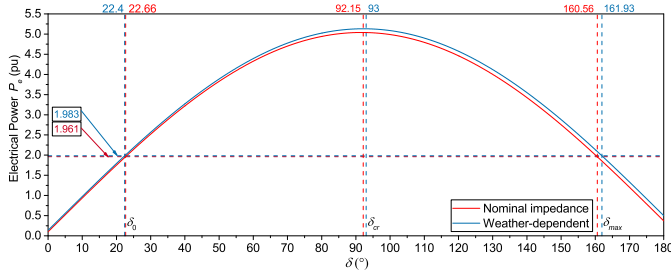


Fig. 5: Power-angle curve on day 35 (80 km length and 250 MVA load).

The calculated critical clearing time of 280.44 ms is also validated by simulating the rotor swing curve of the generator. Figure 6 presents the stable and unstable swing curves of the generator. The unstable curve was obtained when the fault was not cleared until 281.44 ms i.e. 1 ms after the critical clearing time, whereas the stable curve is obtained when the fault is cleared at 279.44 ms. Clearing the fault at 281.44 ms causes the rotor angle to increase rapidly causing loss of synchronism while the fault cleared at 279.44 ms renders the system stable, retaining synchronism.

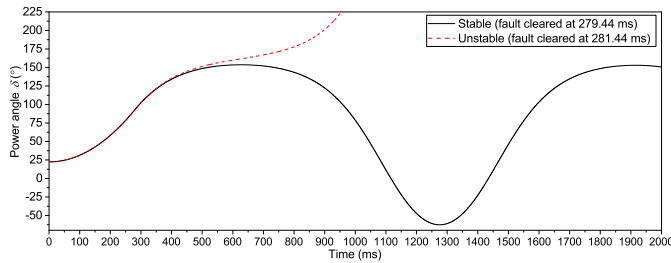


Fig. 6: Rotor swing curve on day 35 (80 km length and 250 MVA load) with fault cleared before and after critical clearing time based on weather-dependent TSA.

A. Impact of loading and transmission line length on weather-dependent TSA

It is important to understand how the loading of the SMIB system and the transmission line length influence the stability indicators from a weather-dependent TSA.

For the investigation, two different loading scenarios are considered i.e. 250 MVA and 500 MVA while the transmission line length is varied from 1 km to 100 km by 1 km increments. The weather conditions considered for this simulation represent the annual mean of the year 2016, which is presented in Table II.

TABLE II: Weather condition

Parameter	Value
T_a ($^{\circ}\text{C}$)	13.2
Q_s (W/m^2)	131
V_s (m/s)	3.51
W_{angle} ($^{\circ}$)	59.96

Figure 7 presents the critical clearing angle and time for the scenario versus different line lengths at 250 MVA loading. As

the line length increases, the transient stability of the system is affected with a decreasing critical clearing angle and time. However, the difference in stability indicators between the nominal impedance scenario and weather-dependent scenario increases with increasing line length. This is because the weather impacts the power flow by impacting the real loss in the transmission lines, which is supplied by the generator. This shifts the initial pre-fault steady-state operating point resulting in the differences observed.

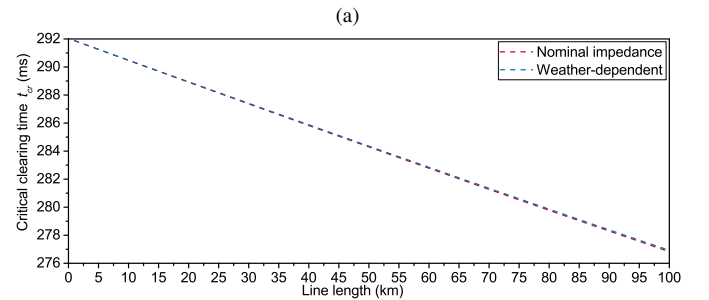
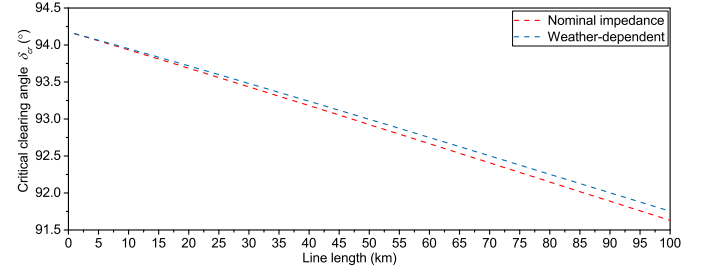


Fig. 7: Critical clearing angle (a) and time (b) versus line length for 250 MVA load. In (b), the weather-dependent critical clearing time is higher at increased line length.

The maximum change was observed at the longest length of 100 km. The maximum absolute change in critical clearing angle for the nominal impedance scenario was 0.12° and the maximum absolute change in critical clearing time for the nominal impedance scenario was 0.09 ms, when compared to the weather-dependent scenario.

The same investigation is repeated again with double the loading (500 MVA) in the network and the stability indicators are presented in Figure 8. As the line length increases for the loaded system, both critical clearing angle and time are lower in Figure 8 as compared to Figure 7. This is due to the real power input by the generator at the pre-fault steady-state condition being higher to meet the higher load. As a result, when the fault occurs, the accelerating power is much higher, which results in rapid acceleration of the rotor resulting in a reduction of the critical clearing angle and time. This is understood by considering the power-angle curve where higher loading means higher pre-fault steady-state power i.e. the overall area under the power-angle curve is reduced resulting in the decreased stability indicators (refer Figure 5 as an example). Furthermore, the difference between the nominal impedance scenario and the weather-dependent scenario is

observed to be greater because of the increased impact of the weather due to higher loading [8].

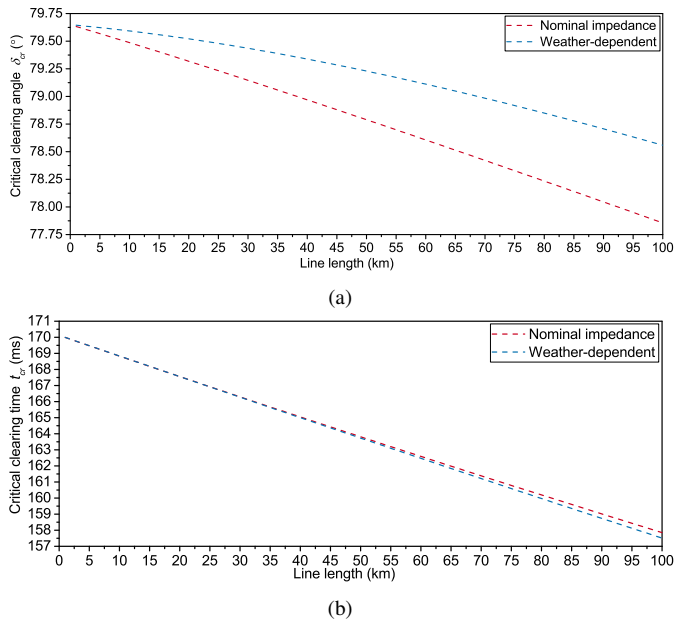


Fig. 8: Critical clearing angle (a) and time (b) versus line length for 500 MVA load.

For the loaded scenario, the absolute change in critical clearing angle at 100 km was 0.7° for the nominal impedance scenario and the absolute change in critical clearing time at 100 km was 0.34 ms for the nominal impedance scenario, when compared to the weather-dependent scenario.

The differences in critical clearing angle and time between the nominal impedance scenario and the weather-dependent scenario in this investigation are observed to increase as both the loading and the line length increased. It is, therefore, expected that under changing weather condition and loading or different transmission line characteristics (resistance, thickness, etc.), the differences could be contributing significantly to TSA.

B. Results Summary & Discussion

In summary, the simulation study demonstrates the impact of weather conditions on TSA and highlights the effect on the two stability indicators (critical clearing angle (δ_{cr}) and time (t_{cr})). In addition, a way to incorporate commonly available weather measurements into TSA is also presented. The simulation study of the SMIB system based on weather-dependent TSA using equal-area criterion in comparison to the traditional nominal impedance scenario presents the benefits of accounting the weather conditions in TSA. The weather-dependent TSA highlights that the critical clearing angle and time of an SMIB system is constantly changing with the changing weather conditions, which indicates power system protection issues that can be improved by considering weather-dependent analysis. Furthermore, it is observed that the weather conditions that result in increased conductor

temperature and resistance of the network lines affect the X/R ratio of the system, which also impacts the critical clearing angle and time. As a result, the weather condition is expected to be a significantly beneficial consideration for power system stability studies to perform accurate analysis as demonstrated by the simulation study, which will improve the power system stability and protection studies.

VI. CONCLUSION

The weather-dependent TSA approach demonstrated in this manuscript presents a framework for accurate transient stability study of SMIB systems incorporating readily available and measured weather conditions by the utilisation of the nonlinear heat balance model of IEEE Std 738TM-2012. Future work entails looking at multi-machine transient stability analysis using the proposed approach.

ACKNOWLEDGMENT

This work was financially supported by the Singapore National Research Foundation under its Campus for Research Excellence And Technological Enterprise (CREATE) programme.

REFERENCES

- [1] O. Elgerd, *Electric Energy Systems Theory: An Introduction*. Tata McGraw-Hill, 1983.
- [2] H. Saadat, *Power System Analysis*. PSA Publishing, 2010.
- [3] J. Glover, M. Sarma, and T. Overbye, *Power System Analysis and Design*. Cengage Learning, 2011.
- [4] P. Kundur, *Power System Stability and Control*, 1st ed. McGraw-Hill, 1994.
- [5] F. Milano, Ed., *Advances in Power System Modelling, Control and Stability Analysis*, ser. Energy Engineering. Institution of Engineering and Technology, 2016.
- [6] B. Stott, "Power system dynamic response calculations," *Proceedings of the IEEE*, vol. 67, no. 2, pp. 219–241, Feb 1979.
- [7] Charles Ventura, "Most of Puerto Rico still in the dark after power plant fire," <https://www.usatoday.com/story/news/2016/09/22/puerto-rico-power-outage-electricity-plant/90823454/>, Sep. 2016.
- [8] A. Ahmed, F. J. Stevens McFadden, and R. K. Rayudu, "Weather-dependent power flow algorithm for accurate power system analysis under variable weather conditions," *IEEE Transactions on Power Systems*, pp. 1–1, 2019.
- [9] A. Ahmed, F. S. McFadden, and R. Rayudu, "Transient stability study incorporating weather effects on conductors," in *2018 IEEE Power & Energy Society General Meeting (PESGM)*. IEEE, 2018, pp. 1–5.
- [10] A. R. Al-Roomi and M. E. El-Hawary, "Effective weather/frequency-based transmission line models - part II: Prospective applications," in *Electrical Power and Energy Conference (EPEC), 2017 IEEE*. IEEE, 2017, pp. 1–8.
- [11] S. Frank, J. Sexauer, and S. Mohagheghi, "Temperature-dependent power flow," *IEEE Transactions on Power Systems*, vol. 28, no. 4, pp. 4007–4018, Nov. 2013.
- [12] "IEEE standard for calculating the current-temperature relationship of bare overhead conductors," *IEEE Std 738-2012 (Revision of IEEE Std 738-2006 - Incorporates IEEE Std 738-2012 Cor 1-2013)*, pp. 1–72, Dec. 2013.
- [13] CIGRE Working Group 22.12, "Thermal behaviour of overhead conductors," *Technical Brochure 207*, 2002.
- [14] M. Pavella, D. Ernst, and D. Ruiz-Vega, *Transient stability of power systems: a unified approach to assessment and control*. Springer Science & Business Media, 2012.
- [15] Y. Zhang, L. Wehenkel, and M. Pavella, "Sime: A comprehensive approach to fast transient stability assessment," *IEEE Transactions on Power and Energy*, vol. 118, no. 2, pp. 127–132, 1998.
- [16] A. Z. Khan, "Effects of power system parameters on critical clearing time: comprehensive analysis," *Electric power systems research*, vol. 49, no. 1, pp. 37–44, 1999.